Antarctic Science 12 (1): 69–79 (2000) © British Antarctic Survey Printed in the United Kingdom

Snow and blue-ice distribution patterns on the coastal Antarctic Ice Sheet

GLEN E. LISTON[1], JAN-GUNNAR WINTHER[2], ODDBJØRN BRULAND[3], HALLGEIR ELVEHØY[4], KNUT SAND[3] and LARS KARLÖF[2]

[1]Department of Atmospheric Science, Colorado State University, Fort Collins, CO 80523, USA
[2]Norwegian Polar Institute, N-9296 Tromsø, Norway
[3]SINTEF Norwegian Hydrotechnical Laboratory, N-7034 Trondheim, Norway
[4]Norwegian Water Resources and Energy Administration, N-0301 Oslo, Norway

Abstract: Surface patterns of alternating snow and blue-ice bands are found in the Jutulgryta area of Dronning Maud Land, Antarctica. The snow-accumulation regions exist in the lee of blue-ice topographic ridges aligned perpendicular to winter winds. The snow bands are *c.* 500–2000 m wide and up to several kilometres long. In Jutulgryta, these features cover *c.* 5000 km^2. These alternating snow and blue-ice bands are simulated using a snow transport and redistribution model, SnowTran-3D, that is driven with a winter cycle of observed daily screen-height air temperature, humidity, and wind speed and direction. The snow-transport model is coupled to a wind model that simulates wind flow over the relatively complex topography. Model results indicate that winter winds interact with the ice topographic features to produce alternating surface patterns of snow accumulation and erosion. In addition, model sensitivity simulations suggest that subtle topographic variations, on the order of 5 m elevation change over a horizontal distance of 1 to 1.5 km, can lead to snow-accumulation variations that differ by a factor of six. This result is expected to have important consequences regarding the choice of sites for ice-coring efforts in Antarctica and elsewhere.

Received 12 July 1999, accepted 2 November 1999

Key words: blue ice, ice coring, snow accumulation, snow distribution, wind

Introduction

The majority of the Antarctic landscape consists of large snow-accumulation areas where glacier and ice sheet mass balance is positive under current climatic conditions. However, in the near-coastal Jutulgryta area of Dronning Maud Land (Fig. 1), alternating patterns of positive and negative mass balance exist. The negative mass-balance areas are usually seen in the form of exposed blue ice that consists of large ice grains up to 1 cm in diameter. The positive mass-balance areas are regions of enhanced snow deposition, where snow deposits lie on top of the blue ice and accumulate to depths of up to several metres. The Jutulgryta area includes regions of gently rolling ice topography that have ridge-to-valley distances of 1–4 km, with ridge-to-valley heights of *c.* 100 m. During winter, the region appears to experience strong and persistent easterly winds (König-Lando *et al.* 1998) that generally keep the blue-ice surfaces swept free of snow accumulations (Takahashi *et al.* 1988, Van den Broeke & Bintanja 1995). The combination of easterly winds and rolling ice-surface topography leads to snow-drift-accumulation zones that form in the lee of the ice hills during winter. These snow-covered areas are found adjacent to the blue-ice fields in the form of bands 500–2000 m wide and up to several kilometres long (Fig. 2). In Jutulgryta about 30% of the region is snow-covered, with similar patterns covering *c.* 5000 km^2.

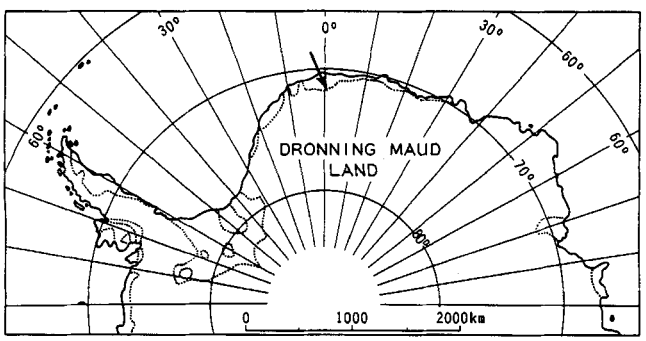

Fig. 1. Location of the Norwegian Antarctic Research Expedition (NARE) study area in Jutulgryta, Dronning Maud Land, Antarctica.

These snow and blue-ice patterns are large and distinct enough to be seen in satellite-based SPOT, AVHRR, and Landsat imagery (Fig. 3), and they provide a striking visual image of the spatial mass-balance variations in this area. In Antarctic regions where blue-ice is not found at the surface, other studies have noted important spatial mass-balance variations occurring at *c.* 5–15 km spatial scales (Black & Budd 1964, Gow & Rowland 1965). Richardson *et al.* (1997), as part of a western Dronning Maud Land snow-distribution mapping study, found that wind redistribution of snow has a significant influence on local accumulation patterns; over distances of less than 5 km, the snow layer thickness varied

https://doi.org/10.1017/S0954102000000109 Published online by Cambridge University Press

Fig. 2. Oblique aerial photograph of snow and blue-ice patterns in the Jutulgryta area of Dronning Maud Land, Antarctica. The large snow stripe in foreground is *c.* 500 m wide by 5 km long. The snow bands are oriented perpendicular to the easterly (from top-left corner) winds. The dark band in the foreground is an ice-covered lake

± 60–70% from the local average value. The strong relationships between local topography, wind, and snow accumulation patterns were also noted by Melvold *et al.* (1998) in the Jutulstraumen area of Antarctica. They found snow accumulation variations of up to 100% over distances of less than 3 km, and attributed these to wind-speed differences associated with changes in surface topography.

Jutulgryta was first visited in February 1990 during the 1989–90 Norwegian Antarctic Research Expedition (NARE), and later studied using a Landsat Thematic Mapper (TM) image recorded on 12 February 1990 (Winther 1993). During NARE 1993–94 the area was revisited for a period of four weeks (e.g. Bøggild *et al.* 1995, Winther *et al.* 1996), and again for five weeks during NARE 1996–97. The 1996–97 study area and field camp is located at 71°24'S, 0°31'E, at *c.* 150 m above sea level (Fig. 1). The snow and ice in this area is *c.* 500 m thick (J.O. Näslund, personal communication 1997).

The blue-ice areas of this region continually experience below-surface melting during the summer months; this generally occurs while the air and surface temperatures are below freezing. The melting can be explained largely by the interactions between the snow-ice-water matrix and the near-surface radiation and energy balances. The low scattering coefficients, that exist in the relatively large-grained blue ice, allow short-wave solar radiation to penetrate the ice. This below-surface energy source, when balanced with the conduction, long-wave, and turbulent energy flux contributions, is sufficient to warm and melt the ice. The adjacent snow-accumulation areas have much higher scattering coefficients and consequently limit solar radiation penetration. In contrast to the below-surface meltwater produced in the blue-ice areas,

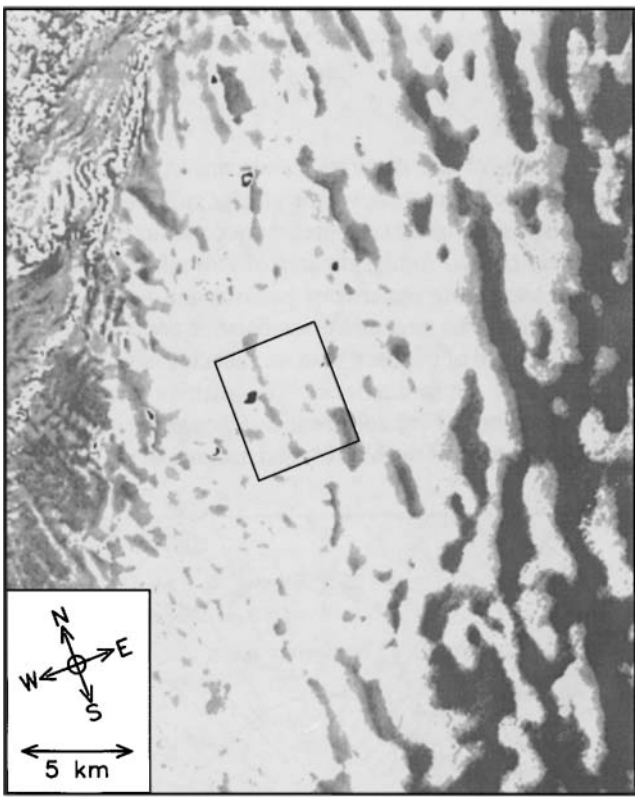

Fig. 3. Landsat Thematic Mapper image collected on 24 January 1986. White areas correspond to blue ice, and grey shades correspond to snow accumulation areas. The inset box is the model simulation domain, and the black areas of the image correspond to ice-covered lakes.

https://doi.org/10.1017/S0954102000000109 Published online by Cambridge University Press

below-surface melting in the nearby snow areas is minimal. A detailed analysis of the thermal and radiative differences between these snow and blue-ice areas is provided by Liston *et al.* (1999). In Antarctica, blue-ice areas at elevations greater than 750 m rarely experience significant melting (Bintanja 1999).

To help describe and explain the snow accumulation and erosion patterns observed in Jutulgryta, a physically-based numerical snow-transport model, SnowTran-3D (Liston & Sturm 1998) has been applied to the area. SnowTran-3D is driven with a winter cycle of observed daily screen-height air temperature, humidity, and wind speed and direction. The snow-transport model is coupled to a wind model that simulates wind flow over the relatively complex topography. The model results indicate that winter winds interact with the ice topographic features to produce alternating patterns of snow accumulation and erosion. The modelling system, and its validation, make use of field observations collected during NARE 1996–97.

In addition to reproducing the observed Jutulgryta snow-distribution patterns, SnowTran-3D will be used to explore the sensitivity of the snow-depth distributions to much more subtle topographic variations than those found in Jutulgryta. This sensitivity simulation will be used to assess whether small topographic variations, on the order of 5 m vertical change over 1 km horizontal distance, might lead to snow-accumulation differences that should be considered when choosing ice-coring sites in areas like Antarctica and Greenland.

Model description

SnowTran-3D has been formulated to simulate the snow-depth evolution over topographically-variable terrain. The model was originally developed and tested in an Arctic-tundra landscape, but is generally applicable to other treeless areas characterized by sufficiently strong winds, low temperatures, and snow precipitation. SnowTran-3D is fully three-dimensional; it is implemented in two horizontal dimensions (x and y), and evolves the snow depth (the z dimension) over a topographically-variable domain. It considers only non-equilibrium transport from the perspective of spatially accelerating and decelerating flow; non-equilibrium transport resulting from temporal wind-speed accelerations and decelerations are not accounted for. The model is applicable to horizontal domains ranging from several tens of metres to a few hundred kilometres on a side. The topography within the domain can vary from flat, to gently rolling, to highly varying, such as regions where flow separation might occur over sharp ridges, gullies, or valleys.

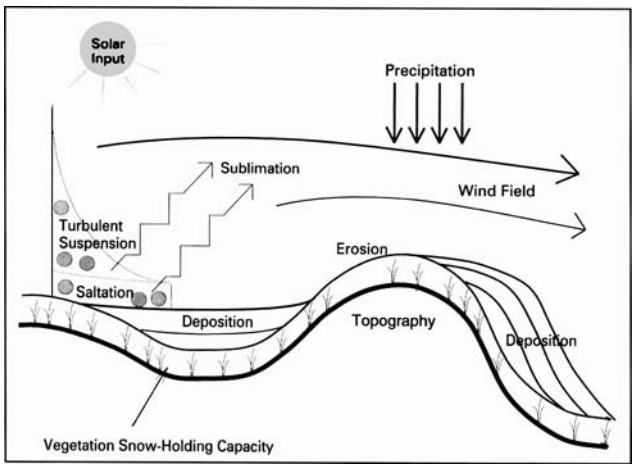

Fig. 4. Key features of the SnowTran-3D snow-transport model applied to topographically-variable terrain (Liston & Sturm 1998).

Figure 4 illustrates the key input parameters (solar radiation, precipitation, wind speed and direction, air temperature, humidity, topography, vegetation (or surface) snow-holding capacity), the key processes (saltation, turbulent-suspension, sublimation), and the key outputs (spatial distribution of snow erosion and deposition) from the model. The six primary components of the snow-transport model are:

1) the computation of the wind-flow forcing field,
2) the wind-shear stress on the surface,
3) the transport of snow by saltation,
4) the transport of snow by turbulent-suspension,
5) the sublimation of saltating and suspended snow, and
6) the accumulation and erosion of snow at the snow surface.

The foundation of this snow-transport model is a mass-balance equation which describes the temporal variation of snow depth at a point. Deposition and erosion, which lead to changes in snow depth at this point are the result of

1) changes in horizontal mass-transport rates of saltation, Q_s (kg m^{-1} s^{-1}),
2) changes in horizontal mass-transport rates of turbulent-suspended snow, Q_t (kg m^{-1} s^{-1}),
3) sublimation of transported snow particles, Q_v (kg m^{-2} s^{-1}), and
4) the water-equivalent precipitation rate, P (m s^{-1}).

Combined, the time rate of change of snow depth, ζ (m), is

$$\frac{d\zeta}{dt} = \frac{1}{\rho_s}\left(\rho_w P - \left(\frac{dQ_s}{dx} + \frac{dQ_t}{dx} + \frac{dQ_s}{dy} + \frac{dQ_t}{dy}\right) + Q_v\right), \quad (1)$$

where t (s) is time; x (m) and y (m) are the horizontal coordinates in the west-east and south-north directions, respectively; and ρ_s and ρ_w (kg m^{-3}) are the snow and water

https://doi.org/10.1017/S0954102000000109 Published online by Cambridge University Press

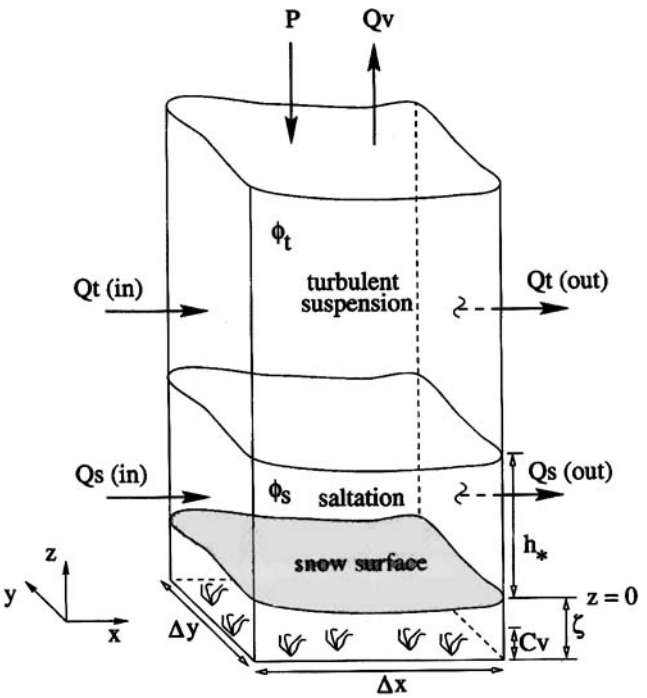

Fig. 5. Schematic of the SnowTran-3D snow-transport model mass-balance computation (Liston & Sturm 1998).

density, respectively. Figure 5 provides a schematic of this mass-balance accounting. Equation 1 is solved for each individual grid cell within a domain, and is coupled to the neighboring cells through the spatial derivatives (*d/dx, d/dy*). In this model formulation we have assumed that the sublimation to or from a static surface (no blowing snow) is negligible. This assumption is supported by observations at Halley research station (75°35'S, 26°19'W) that indicate insignificant (less than 2% of the precipitation) winter sublimation from the snow surface (King *et al.* 1996). Van den Broeke (1997) compared modelled and observed sublimation in Antarctica, and showed that winter sublimation rates are significantly less than summer rates, and that, in certain regions, significant sublimation may occur in spite of the low winter temperatures. Additional details of the formulation of each term in Eq. 1 can be found in Liston & Sturm (1998).

To drive the snow-transport model, a reference-level wind-flow field over the domain of interest is required at each model time step. This wind field is generated by providing an initial distribution in the form adopted by Liston & Sturm (1998), and then applying the continuity-based wind model of Ross *et al.* (1988). Liston & Sturm (1998) took observed wind speeds and directions, and interpolated them to the model grid. These observations are assumed to represent the regional-scale flow regime; in the case of the current study, they represent the combined influence of synoptic and katabatic forcing. This wind field is then modified to account for local topographic influences on the mean flow, by multiplying with an empirically-based weighting factor, *W*,

$$W = 1.0 + \gamma_s \Omega_s + \gamma_c \Omega_c, \qquad (2)$$

where Ω_s and Ω_c are the topographic slope and curvature, respectively, in the direction of the wind, and γ_s and γ_c are positive constants which weight the relative influence of Ω_s and Ω_c on modifying the wind speed. The slope and curvature are computed such that lee and concave slopes produce Ω_s and Ω_c less than zero, and that windward and convex slopes produce Ω_s and Ω_c greater than zero. Thus, lee and concave slopes produce reduced wind speeds, and windward and convex slopes produce increased wind speeds. The resulting wind field is then processed using the NUATMOS wind model of Ross *et al.* (1988) to ensure that the wind field satisfies mass-continuity. In choosing to use NUATMOS, we are taking advantage of that model's ability to suppress the vertical component of the wind field, and thus in some way account for stability of the winter wind field. The model's sensitivity to the NUATMOS stability-parameter value will be discussed later in this paper.

Computational results

Observational data-sets

The snow-transport model was applied to a 5 km by 5.8 km subregion of Jutulgryta that is coincident with a 100-m gridded topographic data-set developed as part of NARE 1996–97. This topography data-set was generated by continuously reading two Ashtech Z-12 dual-frequency global positioning system (GPS) receivers, operating in differential mode and having an accuracy of order 1–2 cm in *x*, *y*, and *z*. One of the receivers was located over a reference stake at the Jutulgryta field camp. The other receiver was mounted on a sled and pulled with a snowmobile along parallel lines *c.* 250 m apart. The measurement interval along these lines depended upon snowmobile speed and averaged *c.* 20 m. The surface topography of all dominant ridges and valley bottoms were also measured. The Jutulgryta-camp reference stake was related to a fixed geodetic-height profile stake at Troll, the Norwegian Antarctic research station located at 72°0'S, 2 31'E. The GPS measurements were related to sea level by comparing the elevation of the Troll reference stake (ellipsoidal height) and Jutulgryta reference stake (open sea water). The difference of 11.3 m was then subtracted from all of the observed Jutulgryta elevations. These observations (*c.* 6400 points) of *x*, *y*, and *z* coordinates where then gridded to the Zone 31 UTM grid at an interval of 100 m using a kriging interpolation procedure (Deutsch & Journel 1998). The accuracy of the topographic elevations in the data-set are assumed to be 1–2 m.

The air temperature, relative humidity, and wind-speed data required to perform the snow-transport model integrations were obtained from the relatively near-by German Neumayer Antarctic research station, located at 70°40'S, 8°15'W, at an elevation of *c.* 40 m above sea level (the Jutulgryta research

https://doi.org/10.1017/S0954102000000109 Published online by Cambridge University Press

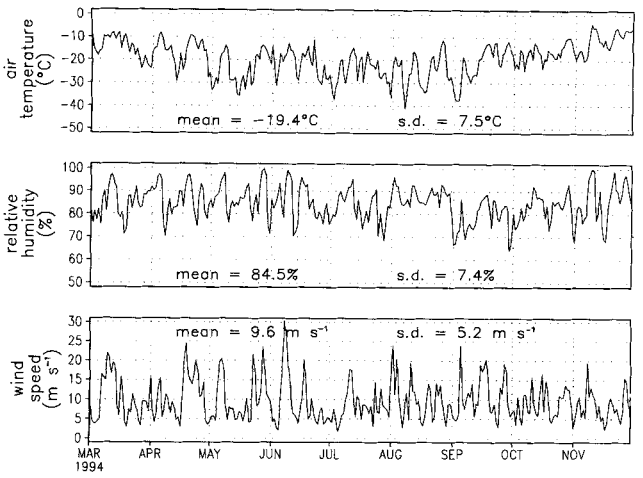

Fig. 6. Daily atmospheric forcing used in the model simulations. Also shown are the mean and standard deviation (s d). These data were collected at the German Neumayer Antarctic research station, and made available as part of the World Meteorological Organization (WMO) World Weather Watch Program (http://www.ncdc.noaa.gov). The wind direction was fixed at 80° east of north.

site is *c.* 85 km north, 315 km east, and 110 m higher than the Neumayer station). A general comparison of 1994–95 data from this station was made with the limited meteorological data collected between 12 January and 9 February 1997 at the Jutulgryta research site. Neumayer was found to be moister and windier, and the average Neumayer air temperature was found to be within 1°C of the average of the Jutulgryta temperature during this 4-week summer period. The Neumayer data-set has been assumed to be fairly representative of the conditions found in Jutulgryta, and the only adjustment made to the Neumayer data was to reduce the air temperatures by 1°C to account for the elevation difference.

Wind direction data are also required to run SnowTran-3D. In a study of the general climatology of Neumayer station, König-Lando *et al.* (1998) found that when winds come from 80 to 90° they are the result of synoptic disturbances and typically have speeds of around 13 m s^{-1}, and winds from 180° are katabatic in origin and have speeds of around 5 m s^{-1}. These katabatic wind speeds are at the threshold required to transport snow, 4–6 m s^{-1} (see Liston & Sturm 1998). Since all snow transport-related features (such as sastrugi and accumulated snow drifts) observed in Jutulgryta indicate a wind direction of 80° (± 10), this suggests that the wind speeds of sufficient magnitude to transport snow (and create the observed features) are of synoptic origin; there were no indications of snow-transporting winds from any other directions.

To get a feel for the potential strength and direction of any katabatic winds occurring in Jutulgryta, the katabatic flow model of Ball (1960), Takahashi *et al.* (1988), and Van den Broeke & Bintanja (1995) was applied using the following inputs: friction coefficient = 1.25×10^{-5} m^{-1}, inversion strength = 5°K, surface temperature = 255°K, Coriolis parameter = 1.382×10^{-4} m^{-1}, and a surface-slope angle of 10 m km^{-1} obtained from the Norwegian Polar Institute 1:250 000 scale "H5S Jutulgryta" satellite image and topographic map. The map indicates that this slope is representative of the region 50 km up-slope from the Jutulgryta research site, and is thus expected to yield a reasonable katabatic wind calculation for the site. This computation yields a katabatic wind speed of 10.9 m s^{-1} and a direction of 39° left of the *c.* 135° downward-pointing surface-slope vector. Thus, the katabatic wind direction in this region is expected to be around 96°. This direction is consistent with our 80° (± 10°) drift-feature observations, and also suggests that any katabatic flow will reinforce the general synoptic conditions based on the König-Lando *et al.* (1998) Neumayer wind speed and direction analyses. Without surface temperature and temperature profile data at Jutulgryta, it is not possible to compute the temporal evolution of the katabatic forcing influences on the wind speed. Thus, the Neumayer wind speeds are used without any modification, under the assumption that they are generally representative of the temporal wind speed variations of the region. These regional-scale winds are then modified, using Eq. 2, to account for local topographic variations. Later in the paper we will discuss additional aspects of the area's wind regime and the sensitivity of the results to using Neumayer data to drive the snow-transport model.

In light of its more coastal location and distance from the Jutulgryta site, the use of air temperature, relative humidity, and wind-speed data from Neumayer is a significant approximation; unfortunately, no other suitable data-set is available. The only Jutulgryta atmospheric-related data used in the model simulations is the drift-feature orientation observations that were made. Based on these observations, the model simulations used a wind-direction of 80°. The model simulations span the period 1 March–30 November 1994. The 275-day, daily-averaged screen-height air temperature, relative humidity, and wind-speed used to drive the model simulations are provided in Fig. 6.

Additional model input is required in the form of snow precipitation. Since this is largely unknown, an arbitrary 0.5 mm of snow-water-equivalent precipitation was assumed to fall each day during the simulation, or a total of *c.* 14 cm snow-water-equivalent over the simulation period. Because this value is so arbitrary, the model-simulated snow distributions will be presented as a ratio of snow depth to precipitation (expressed as a percent), thus highlighting areas of accumulation (values greater than 100%) and erosion (values less than 100%).

Three kinds of snow-pattern distribution observations are used to validate the snow-transport model output. These are

1) oblique aerial photographs taken from a helicopter (e.g. Fig. 2),

2) the snow and blue-ice patterns seen in Fig. 3 1986 Landsat TM image, and

https://doi.org/10.1017/S0954102000000109 Published online by Cambridge University Press

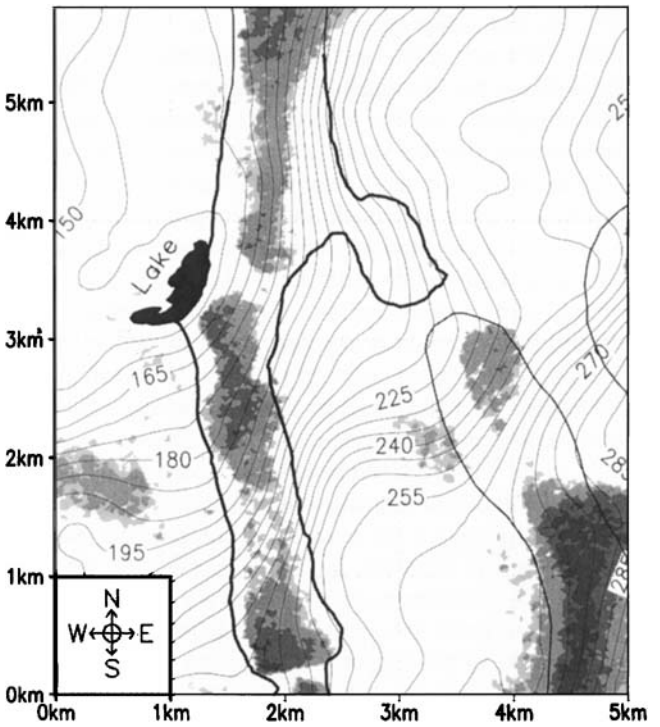

Fig. 7. A detailed view of the model-simulation domain corresponding to the Fig. 3 inset box. Shown are the Landsat image data (grey shades); an ice-covered lake; the topographic distribution (contour interval 5 m, thin black lines); measured snow distribution boundaries (thick black lines); and the snow distribution boundaries, estimated from aerial photographs, for regions not directly measured (medium black lines).

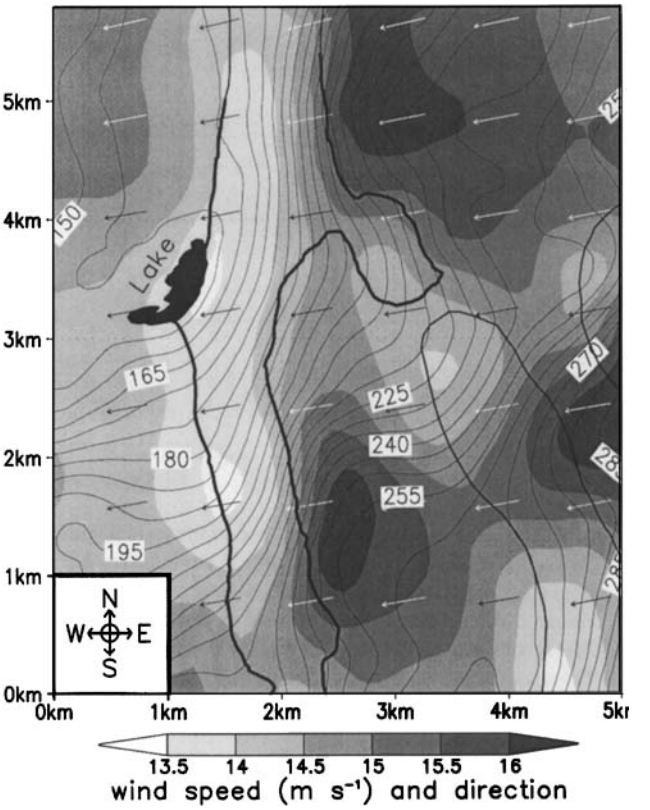

Fig. 8. Example model-simulated wind speed (grey shades) and direction (arrows) distributions for the conditions of a 15 m s^{-1} mean regional wind speed such as those defined in Fig. 6. Also shown are the geographic details of Fig. 7.

3) land-based GPS mapping of the snow and blue-ice boundaries.

Figure 7 shows the Landsat image pattern (grey-shades), snow and blue-ice boundaries based on GPS observations (thick black lines), snow and blue-ice boundaries approximated using oblique aerial photographs (medium black lines), and topographic distribution (thin black lines). Included in the domain is an ice-covered lake nearly 1 km in length (Fig. 7).

Model validation

A summary of the model parameters used in the simulations is provided in Table I. Parameters describing the physical snow characteristics, such as density and threshold wind-shear velocity, have been taken from Arctic Alaska winter snow observations (Liston & Sturm 1998). An example wind-flow field is given in Fig. 8. This represents the topographically-modified wind distribution at a single model time step for the conditions of a 15 m s^{-1} mean regional wind speed such as those defined in Fig. 6. Along the wind-flow direction of 80°, the mean topographic trend over the domain shows a general decrease from east to west. Superimposed on this trend are ridges and depressions that lead to relatively high wind speeds on windward slopes and ridge crests, and lower wind speeds on lee slopes and in low-angle areas. The end-of-winter snow distribution pattern is provided in Fig. 9, where the ratio of simulated snow-depth to precipitation is plotted. Snow is found to accumulate on the steepest lee slopes, and these accumulations generally occur in the same patterns as those observed. Regions exist where the wind has eroded the precipitation down to the blue ice, and in other regions over four times (400%) the precipitation input has accumulated on the surface. Subtle inconsistencies between the model and observations do exist, but are considered minor in light of the complexities and assumptions that comprise the simulations. One notable exception is the model-simulated accumulation

Table I. User-defined constants used in model simulations (see Liston & Sturm (1998) for parameter definitions).

C_v	0.0	snow and ice snow-holding capacity (m)
f	500.0	equilibrium fetch distance (m)
u_{*_t}	0.25	threshold wind-shear velocity (m s^{-1})
z_0	0.0001	snow and ice roughness length (m) (King & Turner 1997)
Υ_c	300.0	topographic curvature weighting factor
Υ_s	3.0	topographic slope weighting factor
μ	3.0	non-equilibrium saltation transport scaling constant
ρ_s	300.0	snow density (kg m^{-3})
α	0.5	atmospheric stability coefficient

https://doi.org/10.1017/S0954102000000109 Published online by Cambridge University Press

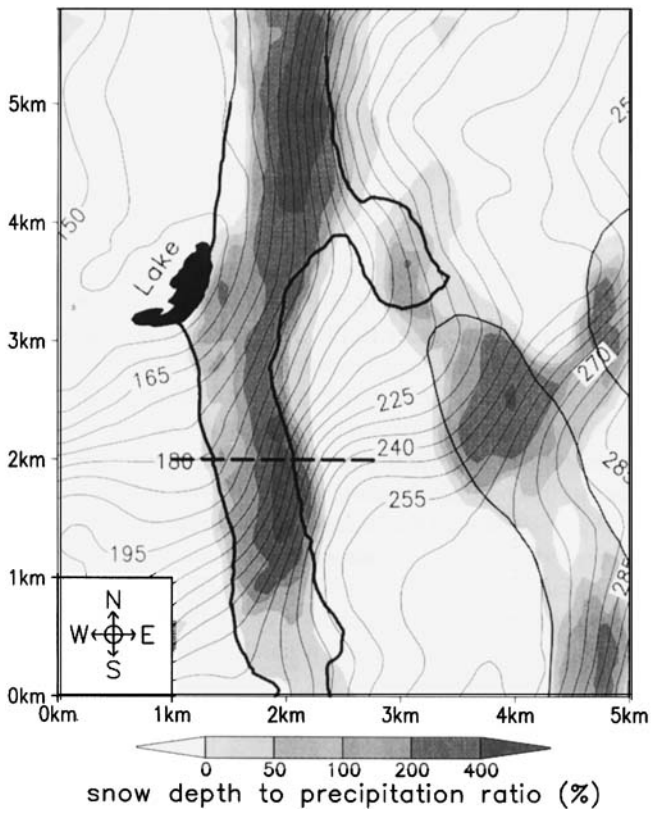

Fig. 9. Model-simulated end-of-winter snow distribution plotted as the ratio of snow depth to total winter precipitation, and expressed as a percent. Thus, values less than 100% indicate erosion, and values greater than 100% indicate deposition. Also shown are the geographic details of Fig. 7 and a dashed line corresponding to the cross-section presented in Fig. 11.

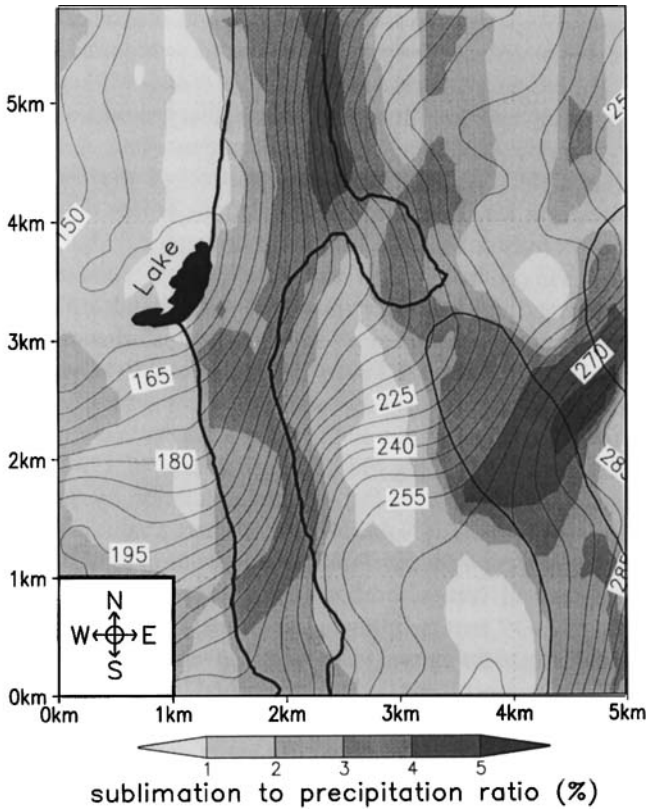

Fig. 10. Model-simulated total-winter sublimation, expressed as a percent of the total winter precipitation (domain mean = 2.3%). Also shown are the geographic details of Fig. 7.

located at *c.* 4.5 km east and 2.5 km north, where snow lies between the two observed snow bands. The topographic contours suggest that this area might well be a significant accumulation zone, but our limited snow-distribution observations in this area do not reflect that; ground-based observations in these steep topographic areas were frequently hindered by the presence of crevasses.

These Jutulgryta accumulation bands are in complete contrast to the slope-change zone depicted in fig. 9, illustration B1, of Takahashi *et al.* (1992), and in fig. 3, illustration III, of Bintanja (1999). In these illustrations, the steeper down-wind slope is characterized by (1) increased wind speeds, (2) erosion, and (3) exposed blue ice. In Jutulgryta, the steeper down-wind slopes are characterized (1) decreased wind speeds, (2) deposition, and (3) snow accumulations that lie over the blue ice. We conclude that there is a definite length-scale dependence upon the character and formation of these different accumulation/erosion zones. The Jutulgryta case is thought to be the result of wind speed variations in response to relatively small-scale, mechanically-forced influences, and the Takahashi *et al.* (1992) case represents conditions produced by wind speed variations resulting from differences in the relatively large-scale katabatic forcing.

The spatial distribution of total-winter moisture returned to the atmosphere by sublimation during snow-transport processes, as simulated by the model (Q_v in Eq. 1), is given in Fig. 10. The model suggests as much as 5% of the winter precipitation sublimates, with a domain mean of 2.3%. This model result is consistent with the findings of King *et al.* (1996) who showed that autumn and winter blowing snow sublimation at Halley, which has a similar climatology to Neumayer (König-Lando *et al.* 1998), equals 1 to 2% of the precipitation. This relatively-low sublimation is in contrast to values computed for Arctic Alaska, where observations and model simulations suggest that locally over 30% of the winter precipitation can sublimate (Liston & Sturm 1998). Comparison of the meteorological forcing used for these Arctic and Antarctic simulations suggests that the reasons for the lower Antarctic sublimation are the lower air temperatures (about 5°C lower) and higher relative humidities (about 10% higher). These two factors more than compensate for the sublimation increase that would normally occur with the greater Antarctic wind speeds (about 5 m s^{-1} greater). Because of its more coastal location, the Neumayer winter relative humidities may be higher than those found in Jutulgryta, thus leading to an underestimate of the computed sublimation. To quantify any potential misrepresentation, actual winter

https://doi.org/10.1017/S0954102000000109 Published online by Cambridge University Press

meteorological observations from Jutulgryta, or another station of similar distance from the coast, would be required.

The NUATMOS wind model of Ross *et al.* (1988) includes an atmospheric stability coefficient, α, that provides a means to suppress the vertical velocity component of the simulated wind field. A significant characteristic of the observed Jutulgryta lee-slope snow accumulations is that they exist significantly down slope from the topographic "ridge" crest. This is in contrast to snow accumulation sites found in other middle and high latitude environments where winds are largely the result of synoptic-scale atmospheric disturbances (e.g. Tabler 1975, Liston & Sturm 1998). In Jutulgryta, we have assumed that the winter winds exist under typically-stable atmospheric conditions and include a katabatic component (e.g. Parish 1988, King 1989, König-Lando *et al.* 1998). This factor is included in the Fig. 9 model simulation, by choosing a relatively arbitrary value of $\alpha = 0.5$, where a value of $\alpha = 1.0$ would represent neutral stability, and a value of $\alpha = 0.0$ would suppress all vertical motion (from the perspective of the NUATMOS terrain-following coordinate system). Model sensitivity to the chosen value of α is given in Fig. 11, for the 1.8-km transect identified by the dashed line in Fig. 9. The total elevation difference from one end of this transect to the other is 64 m. Figure 11 shows that as the stability coefficient is decreased, the position of the drift shifts further down slope in response to the increased stability and suppressed potential for flow separation. In addition, the volume of the drift is reduced because more snow is transported further downwind past the drift.

Subtle topography

The ice-topography variations in the Jutulgryta area are generally greater than the topographic variation found in most Antarctic areas, with the most notable exception being areas around and including nunataks. To address how snow-depth distributions might vary in regions of more subdued topography, the snow-transport model was run again for the same conditions as presented in the Fig. 9 validation simulation, but with the topographic distribution multiplied by a factor of one-tenth. This effectively produced a topographic data-set that has the same distribution pattern as the observed topography, but one with significantly-reduced topographic magnitudes and spatial differences. By leaving all other aspects of the model configuration the same as those used in the original model-validation simulation, we isolate the model's sensitivity to the more subtle topographic distribution. In addition, by preserving the basic model-validation configuration, we are able to take advantage of its general success at accounting for the driving factors that produce the observed Jutulgryta snow distribution.

An example wind field computed for the subdued topography is provided in Fig. 12; also shown is the new topographic distribution and the geographic features from Fig. 7. Figure 12 represents the topographically-modified wind distribution at a single model time step for the conditions of a 15 m s^{-1} mean

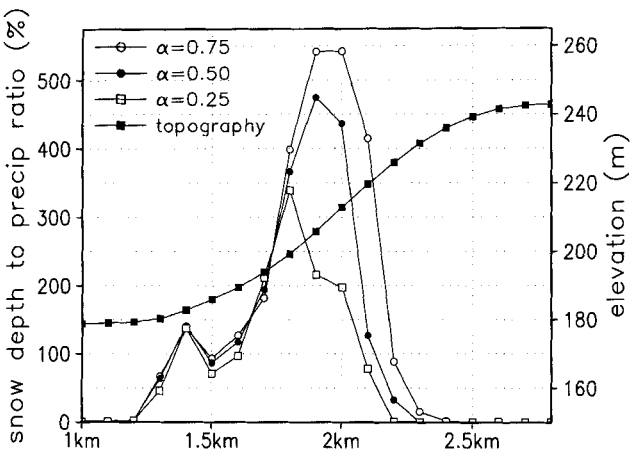

Fig. 11. Sensitivity of the end-of-winter snow distribution to the atmospheric stability parameter, α. Shown is the snow-accumulation profile at a position $y = 2$ km, and between $x = 1.0$ and 2.8 km, corresponding to the dashed line in Fig. 9. Also included is the topographic profile for the same transect.

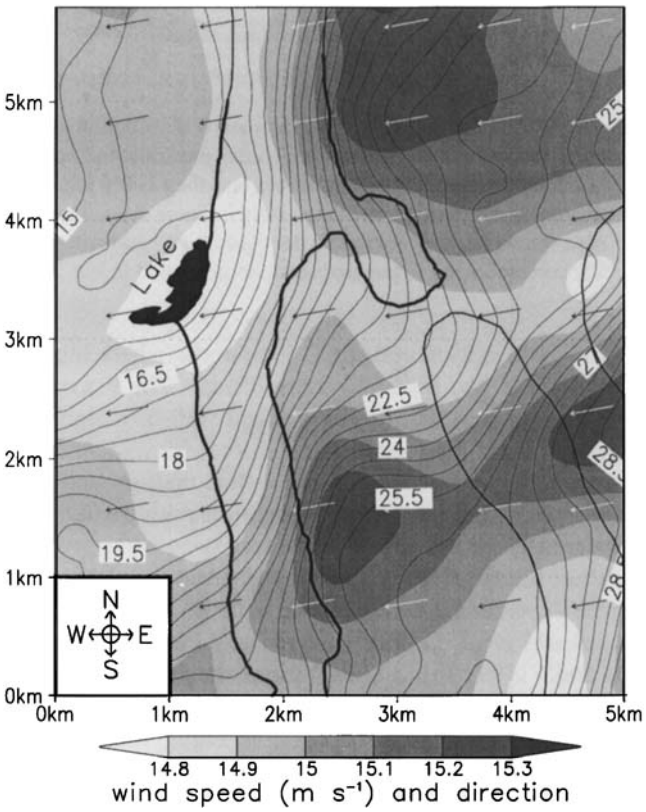

Fig. 12. Example model-simulated wind speed (grey shades) and direction (arrows) distributions for the case of the topographic distribution multiplied by one-tenth, and for the conditions of a 15 m s^{-1} mean regional wind speed such as those defined in Fig. 6. Also shown are the lake and snow and blue-ice boundaries of Fig. 7 and the new topographic distribution (contour interval 0.5 m).

https://doi.org/10.1017/S0954102000000109 Published online by Cambridge University Press

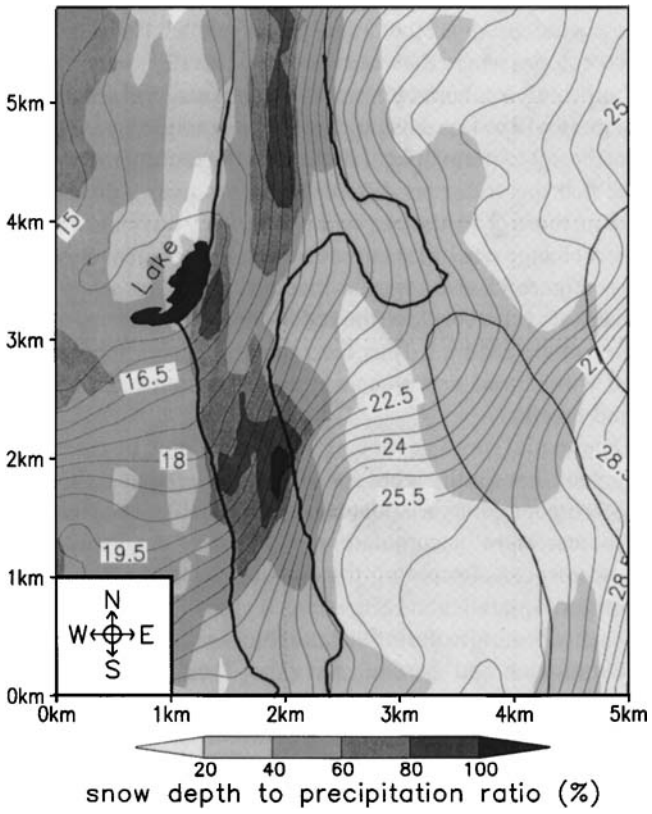

Fig. 13. Model-simulated end-of-winter snow distribution plotted as the ratio of snow depth to total winter precipitation, and expressed as a percent, for the case of the topographic distribution multiplied by one-tenth. Also shown are the geographic details of Fig. 12.

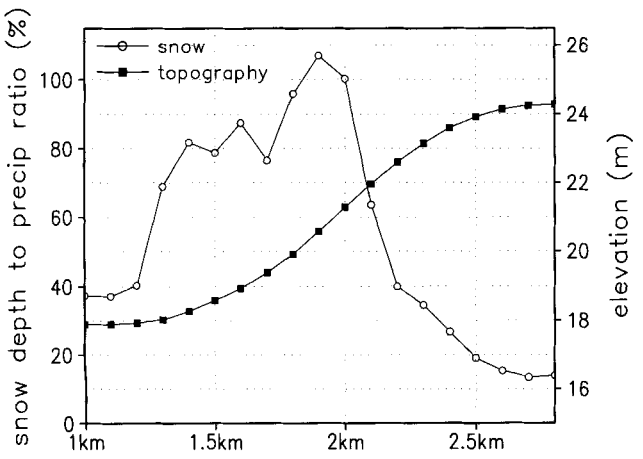

Fig. 14. The snow-accumulation profile at a position $y = 2$ km, and between $x = 1.0$ and 2.8 km, corresponding to the dashed line in Fig. 9, for the case of the topographic distribution multiplied by one-tenth. Also included is the topographic profile for the same transect.

regional wind speed. As such, it can be directly compared with the Fig. 8 wind field. The magnitude of the wind-speed variability is much reduced compared to the validation simulation (Fig. 8), where the validation simulation used a shading interval of 0.5 m s^{-1} and the reduced-topography simulation used a shading interval of 0.1 m s^{-1}. In spite of this reduction in the spatial wind-speed differences, the wind-flow pattern remains very similar. The model-simulated snow distribution is provided in Fig. 13. The snow-distribution pattern is similar to that of the validation simulation (Fig. 9), but the snow-depth magnitudes are quite different. The reduced-topography simulation has produced maximum snow accumulations that roughly equal the precipitation inputs (contour values of 100%), and all other areas represent erosion of the precipitation. Considering the cross-section identified by the dashed line in Fig. 9, the snow depth ratio in Fig. 13 varies from *c.* 15% in the east, to an average of about six times that depth (*c.* 90%) in the main drift-accumulation area (Fig. 14). These snow-depth changes occur over a distance of between 1 and 1.5 km, and correspond to a topographic difference of *c.* 5 m (Fig. 14).

Discussion and conclusions

A numerical snow-transport model has been driven with observed meteorological data and used to successfully simulate, and help understand, the observed snow distribution and blue-ice patterns in the Jutulgryta area of Dronning Maud Land, Antarctica. The initial model simulation has been validated against snow observations. The Jutulgryta area is unique because the snow-distribution patterns are visible from surface and remotely-sensed observations in the form of alternating snow and blue-ice bands. In spite of the success of the model simulations, there are deficiencies in the simulations and analyses that could be addressed if the required observational data-sets were available. To help overcome deficiencies in our snow-transport model input data-sets, such as precipitation and winter snow density, the end-of-winter model results have been presented as a snow depth to precipitation ratio. An additional deficiency in the model-simulation analysis is that we do not know the actual winter snow accumulation for the snow-accumulation sites; we only know the snow and blue-ice boundaries. In spite of these limitations, it is clear that the observed snow and blue-ice patterns are the result of winter winds that interact with the ice-topography and produce alternating surface patterns of snow accumulation and erosion.

An additional assumption used in the simulations is that it is appropriate to use air temperature, relative humidity, and wind speed data from Neumayer to drive the snow-transport model simulations. For the analysis presented herein, where we are only looking at the snow-distribution patterns, the model is not very sensitive to those inputs. Model sensitivity simulations (not shown) were performed where (1) the relative humidities in Fig. 6 were decreased by 25%, and (2) temporally constant wind speeds of 10 and 15 m s^{-1} were used. These

https://doi.org/10.1017/S0954102000000109 Published online by Cambridge University Press

simulations yield similar snow-distribution patterns as those using the Neumayer meteorological data, and suggest that the conclusions presented herein are relatively insensitive to potential misrepresentations in the humidity and wind speed forcing data. However, we find these patterns are very sensitive to the prescribed wind direction, and we believe that our success in simulating the patterns lies in our use of observed Jutulgryta snow features, like sastrugi, to define the wind direction. These simulations also support our general conclusion that the dominant process that leads to the snow accumulation bands is snow erosion and deposition by wind, and not winter spatial variations in sublimation. We have not addressed summer processes like sublimation that may also influence the observed patterns. Our analysis of the simulated depth and sublimation quantities as fractions relative to the precipitation input has provided a qualitative feel for the modeling results, rather than a quantitative assessment of the individual mass balance features of this site. If we were trying to compare modeled snow depths with snow-depth observations, then the inputs of temperature, relative humidity, wind speed, and precipitation would be much more important.

While using the general model-validation configuration, an additional simulation was performed for the conditions of the topographic distribution multiplied by a factor of one-tenth. This subdued-topography simulation showed significant (a factor of six) snow-distribution sensitivity to topographic differences of around 5 m over horizontal distances of less than 1.5 km. The dominant reason why the snow distribution is sensitive to relatively-low spatial topographic and wind-speed variations is the non-linear character of the turbulent-suspended horizontal snow-flux computation (Liston & Sturm 1998). Figure 15 describes the variation of maximum potential saltation and turbulent-suspended transport with wind speed (Q_s and Q_t, respectively, in Eq. 1). The minimum and maximum wind speed contours in Fig. 12 are 14.8 and 15.3 m s^{-1}, respectively, and Fig. 15 shows that the corresponding maximum turbulent-suspended transports for these wind speeds are 0.442 and 0.518 kg m^{-1} s^{-1}. Consequently, on lee slopes where the wind speed is generally lower, there is significantly less horizontal mass flux and snow will accumulate (or there will be less erosion) there. For example, by assuming that the dQ_t/dy term in Eq. 1 dominates the snow mass balance, and that this transport difference occurs over a distance of 600 m, these Q_t values can be input into Eq. 1 to yield a snow-depth change rate of 1.1 cm snow-water-equivalent depth per day. Figure 15 also suggests that during periods when wind speeds are relatively low, the snow-depth change rates will be substantially reduced. Thus, the influence of subtle topographic and wind-speed variations are more pronounced at higher wind speeds.

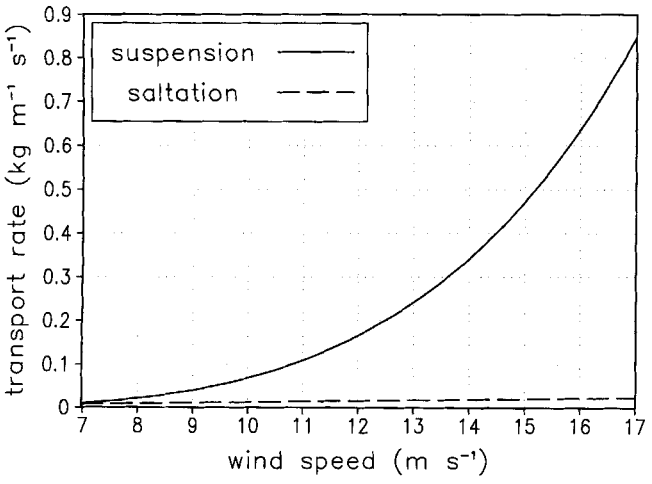

Fig. 15. Variation of saltation and turbulent-suspended transport with screen-height wind speed, for the case of $u_{*_t} = 0.25$ m s^{-1} (Liston & Sturm 1998).

The spatial snow-depth variability simulated by the model suggests that for the wind speeds encountered at Jutulgryta, subtle topographic variations can lead to significant differences in winter snow accumulation. This may have important consequences concerning the choice of sites for ice-coring efforts in Antarctica and elsewhere. Typically, coring sites are chosen to minimize the influence of blowing and drifting snow accumulation and erosion, and other local factors such as prevailing ice-flow directions. The preceding analysis suggests that there may be a significant snow-accumulation sensitivity to topographic variations on the order of several metres per kilometre; variations that may not be obvious when standing on the snow-ice surface. The model simulations suggest that subtle topographic variations, previously assumed to be unimportant, might warrant additional consideration.

In light of these model simulations, we expect that similar snow-depth variability can be expected in other areas of Antarctica where winds are sufficient to transport snow and where there are similar topographic variations. To further understand the wind redistribution of snow throughout Antarctica, an observational data-set that includes the spatial distribution of annual snow accumulation, over a domain of *c.* 100 km^2 and at a resolution of *c.* 100 m, would be invaluable. Topographic data over the same grid are also required, and snow-density observations would allow improved estimates of snow-related characteristics such as the snowcover's threshold wind-shear velocity. In addition, these data-sets need to be combined with winter observations of screen-height air temperature, humidity, and wind speed and direction.

Acknowledgements

The participants of NARE 1996–97 are gratefully acknowledged for their role in making the field programme a success. We would like to particularly acknowledge Bjørn Barstad from the Norwegian Polar Institute Mapping Department; his willingness to support our interest in creating a high-resolution topographic data-set for Jutulgryta, and his substantial efforts to help us collect and process those required data, made this work possible. The authors also thank Drs

John King and Richard Bintanja for their insightful critique of this research and its presentation.

This is publication No. 160 of the Norwegian Antarctic Research Expeditions. This work was funded by the Norwegian Research Council.

References

BALL, F.K. 1960. Winds on the ice slopes of Antarctica. In *Antarctic Meteorology: Proceedings of the Symposium, Melbourne 1959* New York: Pergamon Press, 9–16.

BINTANJA, R. 1999. On the glaciological, meteorological, and climatological significance of Antarctic blue ice areas. *Reviews of Geophysics*, **37**, 337–359.

BLACK, H.P. & BUDD, W. 1964. Accumulation in the region of Wilkes, Wilkes Land, Antarctica. *Journal of Glaciology*, **5**(37), 3–15.

BØGGILD, C.E., WINTHER, J.-G., SAND, K. & ELVEHØY, H. 1995. Subsurface melting in blue-ice fields in Dronning Maud Land, Antarctica: observations and modelling. *Annals of Glaciology*, **21**, 162–168.

DEUTSCH, C.V. & JOURNEL, A.G. 1998. *GSLIB geostatistical software library and user's guide.* New York: Oxford University Press, 369 pp.

GOW, A.J. & ROWLAND, R. 1965. On the relationship of snow accumulation to surface topography at "Byrd Station", Antarctica. *Journal of Glaciology*, **5**(42), 843–847.

KING, J.C. 1989. Low-level wind profiles at an Antarctic coastal station. *Antarctic Science*, **1**, 169–178.

KING, J.C. & TURNER, J. 1997. *Antarctic meteorology and climatology.* Cambridge: Cambridge University Press, 409 pp.

KING, J.C., ANDERSON, P.S., SMITH, M.C. & MOBBS, S.D. 1996. The surface energy and mass balance at Halley, Antarctica during winter. *Journal of Geophysical Research*, **101**(D14), 19 119–19 128.

KÖNIG-LANDO, G., KING, J.C. & PETTRÉ, P. 1998. Climatology of the three coastal Antarctic stations Dumont d'Urville, Neumayer, and Halley. *Journal of Geophysical Research*, **103**(D9), 10 935–10 946.

LISTON, G.E. & STURM, M. 1998. A snow-transport model for complex terrain. *Journal of Glaciology*, **44**(148), 498–516.

LISTON, G.E., WINTHER, J.-G., BRULAND, O., ELVEHØY, H. & SAND, K. 1999. Below-surface ice melt on the coastal Antarctic ice sheet. *Journal of Glaciology*, **45**(150), 273–285.

MELVOLD, K., HAGEN, J.O., PINGLOT, J.F. & GUNDESTRUP, N. 1998. Large spatial variation in accumulation rate in Jutulstraumen ice stream, Dronning Maud Land, Antarctica. *Annals of Glaciology*, **27**, 231–238.

PARISH, T.R. 1988. Surface winds over the Antarctic continent: A review. *Reviews of Geophysics*, **26**(1), 169–180.

RICHARDSON, C., AARHOLT, E., HAMRAN, S.-E., HOLMLUND, P. & ISAKSSON, E. 1997. Spatial distribution of snow in western Dronning Maud Land, East Antarctica, mapped by ground-based radar. *Journal of Geophysical Research*, **102**(B9), 20 343–20 353.

ROSS, D.G., SMITH, I.N., MANINS, P.C. & FOX, D.G. 1988. Diagnostic wind field modeling for complex terrain: model development and testing. *Journal of Applied Meteorology*, **27**, 785–796.

TABLER, R.D. 1975. Predicting profiles of snowdrifts in topographic catchments. *Proceedings of the Western Snow Conference, 43rd Annual Meeting, 23-25 April 1975, Coronado, California*, 87–97.

TAKAHASHI, S., NARUSE, R., NAKAWO, M. & MAC, S. 1988. A bare ice field in east Queen Maud Land, Antarctica, caused by horizontal divergence of drifting snow. *Annals of Glaciology*, **11**, 156–160.

TAKAHASHI, S., ENDOH, T., AZUMA, N. & MESHIDA, S. 1992. Bare ice fields developed in the inland part of Antarctica. *Proceedings of the NIPR Symposium on Polar Meteorology and Glaciology*, **5**, 128–139.

VAN DEN BROEKE, M.R. 1997. Spatial and temporal variation of sublimation on Antarctica: results of a high-resolution general circulation model. *Journal of Geophysical Research*, **102**(D25), 29765–29777.

VAN DEN BROEKE, M.R. & BINTANJA, R. 1995. On the interaction of katabatic wind and blue ice area formation in East Antarctica. *Journal of Glaciology*, **41**, 395–407.

WINTHER, J.-G. 1993. Studies of snow surface characteristics by Landsat TM in Dronning Maud Land, Antarctica. *Annals of Glaciology*, **17**, 27–34.

WINTHER, J.-G., ELVEHØY, H., BØGGILD, C.E., SAND, K. & LISTON, G.E. 1996. Melting, runoff and the formation of frozen lakes in a mixed snow and blue-ice field in Dronning Maud Land, Antarctica. *Journal of Glaciology*, **42**, 271–276.